Neuropsychiatric Disease and Treatment

Dovepress
Taylor & Francis Group

Open Access Full Text Article

ORIGINAL RESEARCH

Investigation on Inhibiting SPHK - S1P Pathway to Improve ADHD Model Rats Behavior via Lipidomics

Dingyue Chai[1], Yuzi Sun[1], Jiamin Lu[1], Yuhui Yao[2], Chunyu Jiang[1], Lihui Wu[1], Qianqian Cai[3]

[1]Departments of Basic Medicine and Forensic Medicine, Hangzhou Medical College, Hangzhou, People's Republic of China; [2]Department of Paediatrics, The First Hospital of Jiaxing, Zhejiang, People's Republic of China; [3]Shanghai Key Laboratory of Molecular Imaging, Jiading District Central Hospital Affiliated Shanghai University of Medicine and Health Sciences, Shanghai, 201318, People's Republic of China

Correspondence: Lihui Wu; Qianqian Cai, Email jaemny@163.com; caiqq@sumhs.edu.cn

Neuropsychiatric Disease and Treatment downloaded from https://www.dovepress.com/
For personal use only.

Purpose: Attention-Deficit/Hyperactivity Disorder (ADHD) is one of the most prevalent neurodevelopmental disorders in childhood, with a globally increasing incidence. This study aims to investigate alterations in prefrontal cortical lipid metabolism in ADHD model rats and following transcutaneous auricular vagus nerve stimulation (taVNS) intervention, and to elucidate the regulatory effects of the sphingosine kinase inhibitor SKI II on the SPHK-S1P signaling pathway.

Methods: Lipidomic analysis was performed to profile the lipid spectrum in prefrontal cortex tissues from Wistar-Kyoto (WKY) control rats, spontaneously hypertensive rat (SHR) ADHD models, sham-operated rats, and taVNS intervention rats. Key sphingolipid metabolic enzymes were assessed by RT-qPCR and Western blot, while sphingosine-1-phosphate (S1P) levels were quantified via ELISA. ADHD model rats received intraperitoneal administration of SPHK inhibitor SKI II (15 mg/kg, 16 days). Behavioral tests evaluated hyperactivity, impulsivity, and anxiety-like phenotypes. Western blot analyzed expression of dopamine synthesis rate-limiting enzyme.

Results: The ADHD model group exhibited significantly elevated ganglioside and lysophospholipid levels. taVNS intervention specifically reduced sphingomyelin content. SPHK1 and SPHK2 mRNA and protein expression were markedly upregulated in ADHD models, concomitant with increased S1P levels. taVNS selectively decreased *Sphk2* mRNA expression (without altering protein levels). SKI II administration significantly ameliorated hyperactivity, impulsivity, and anxiety-like behaviors in ADHD models, concurrently restoring dopamine β-hydroxylase expression.

Conclusion: The SPHK-S1P signaling axis is a core pathway driving sphingolipid metabolic dysregulation in the prefrontal cortex in ADHD. Targeted inhibition of this pathway synergistically modulates the expression levels of proteins associated with dopaminergic neurotransmission. The limited regulatory effect of taVNS on sphingolipid metabolism suggests its clinical benefits may stem from multi-pathway synergistic mechanisms.

Keywords: attention-deficit/hyperactivity disorder, sphingolipid metabolism, SPHK-S1P, taVNS

Introduction

Attention deficit hyperactivity disorder (ADHD) is a neurodevelopmental disorder characterized by persistent hyperactivity, impulsivity, and inattention.[1,2] These core symptoms typically emerge during preschool and often persist into adulthood, significantly impairing learning capacity, social adaptation,[3] and mental health outcomes.[4] Recent global epidemiological data highlight the high prevalence of ADHD in pediatric populations,[5] with estimated rates of 7.6% (95% CI: 6.1–9.4%) among children aged 3–12 years and 5.6% (95% CI: 4.8–7%) in adolescents aged 12–18 years.[6] A pronounced gender disparity exists, with males being disproportionately affected at a 2–4 times higher prevalence than females.[7–9] While gene-environment interactions are widely recognized as contributors to ADHD pathogenesis,[10,11] its molecular mechanisms remain elusive. The classical monoamine hypothesis—primarily attributing symptoms to dysregulation of dopamine/norepinephrine systems[12]—partially explains clinical manifestations but struggles to account for

Received: 26 March 2025
Accepted: 22 August 2025
Published: 10 September 2025

© 2025 Chai et al. This work is published and licensed by Dove Medical Press Limited. The full terms of this license are available at https://www.dovepress.com/terms.php and incorporate the Creative Commons Attribution – Non Commercial (unported, v4.0) License (http://creativecommons.org/licenses/by-nc/4.0/). By accessing the work you hereby accept the Terms. Non-commercial uses of the work are permitted without any further permission from Dove Medical Press Limited, provided the work is properly attributed. For permission for commercial use of this work, please see paragraphs 4.2 and 5 of our Terms (https://www.dovepress.com/terms.php).

the disorder's heterogeneity and variability in treatment responses. This limitation underscores the need to explore complementary biological pathways, such as lipid metabolism, to advance the mechanistic understanding of ADHD etiology.

The relationship between lipid metabolism and neurological disorders has garnered increasing attention recently.[13] As one of the most abundant macromolecules in the brain,[14] lipids regulate neurodevelopment and functional homeostasis through diverse components such as cholesterol, glycerophospholipids, and sphingolipids.[15,16] Specifically, cholesterol serves as a critical constituent for synaptic formation,[17] glycerophospholipids maintain neuronal membrane fluidity and signaling efficiency,[18] while sphingolipids modulate neural plasticity by mediating cell cycle progression, inflammatory responses, and autophagy.[19] Notably, sphingolipid metabolism is pivotal in neurological disorders due to its direct involvement in myelination and synaptic transmission.[20] Emerging clinical evidence suggests abnormal central myelination in ADHD patients.[21] Furthermore, whole-exome genotyping has identified significant correlations between genetic variations in sphingolipid-metabolizing enzyme genes (eg, *GALC, CERS2, CERS6, CERK, SMPD1*) and ADHD susceptibility.[21] This compelling evidence underscores sphingolipid dysregulation as a potential metabolic hub in ADHD pathophysiology.

The sphingolipid metabolic network regulates neural function through the dynamic equilibrium of key enzyme-substrate axes.[22] Ceramide, the central hub of this network, undergoes metabolism via three interconnected pathways: de novo synthesis, salvage pathway, and catabolism.[23] De novo synthesis initiates with the conversion of serine and palmitoyl-CoA into ceramide through sequential enzymatic reactions. The salvage pathway involves ceramide recycling through the hydrolysis of sphingomyelin or glycosphingolipids. Specifically, sphingomyelin phosphodiesterase 1 (SMPD1) hydrolyzes sphingomyelin to ceramide, maintaining their homeostatic balance. Glycosphingolipids are cleaved by glycosidases to release sphingosine or ceramide, while ceramide can also be glycosylated via Golgi-resident transferases to form gangliosides (GM). Hexosaminidase A (HEXA), essential for degrading GM2 to GM3, has been implicated in neurodegenerative pathologies—its deficiency leads to GM2 accumulation, triggering neuronal degeneration and neuroinflammation.[24]

Catabolism involves ceramidase-mediated hydrolysis of ceramide into sphingosine, which is subsequently phosphorylated by sphingosine kinases (SPHK1/SPHK2) to generate sphingosine-1-phosphate (S1P). S1P acts as a bioactive lipid mediator that modulates neuronal excitability and synaptic plasticity,[25] crucially maintaining cerebral functional integrity.[26] Conversely, ceramide synthase 1 (CERS1)—predominantly expressed in the brain—catalyzes sphingosine-to-ceramide conversion, sustaining sphingolipid homeostasis.[27] Notably, CERS1 mutations are directly associated with neuronal apoptosis.[28] Furthermore, ceramide kinase (CERK) phosphorylates ceramide to produce ceramide-1-phosphate (C1P), expanding the functional diversity of sphingolipid signaling.[29] Despite these advances, the dynamic interplay between sphingolipid dysregulation and ADHD behavioral phenotypes remains unexplored. Critical gaps persist in understanding node-specific regulatory mechanisms and validating targeted interventions. Spatial lipidomics emerges as a pivotal tool to resolve region-specific metabolic signatures,[30] offering mechanistic insights for this investigation.

This study proposes a novel scientific hypothesis that dysregulation of the sphingolipid metabolic network may underlie the pathogenesis of ADHD. Building on the neuroregulatory potential of taVNS in metabolic pathways,[31] we utilized spontaneously hypertensive (SHR) rats as a validated animal model for ADHD. This model replicates the core clinical features of human ADHD,[32] including persistent attention deficits, motor impulsivity, and hyperactivity.[33] Wistar Kyoto (WKY) rats were used as normotensive controls. Integrated lipidomic profiling of the prefrontal cortex (PFC), a brain region central to higher-order cognition and neurodevelopmental disorders,[34] was conducted across taVNS-treated, sham-operated, and untreated groups to elucidate metabolic remodeling mechanisms. Untargeted lipidomics identified sphingolipid metabolism as the key dysregulated pathway. Subsequent analyses characterized dynamic enzymatic activity alterations in critical nodes of the sphingolipid network, particularly the SPHK-S1P axis, along with metabolite accumulation patterns. Pharmacological inhibition of sphingosine kinase using SKI II in SHRs demonstrated dual therapeutic effects, attenuating ADHD-like behavioral phenotypes while normalizing molecular signatures of sphingolipid dysregulation. These findings advance a theoretical framework for developing metabolism-targeted interventions.

Materials and Methods

Animals

Specific pathogen-free (SPF) male Wistar-Kyoto (WKY) and spontaneously hypertensive rats (SHR) were obtained from Beijing Vital River Laboratory Animal Technology Co., Ltd. The rats were housed in five per cage under controlled conditions (23 ± 1°C, 50 ± 5% humidity) with ad libitum access to food and water, and maintained on a 12-hour light/dark cycle. After a 7-day acclimation period, the experiments were initiated. We strictly controlled the number of experimental animals to the minimum required for obtaining statistically significant results, thereby reducing potential suffering without compromising scientific validity.

Lipidomics Analysis

Sample Processing

Rats were anesthetized using isoflurane. After performing a craniotomy, the prefrontal cortex was quickly collected and stored at −80°C. For lipid extraction, 200 μL of water and 20 μL of an internal lipid standard mixture were added to the tissue and vortexed. Subsequently, 800 μL of MTBE and 240 μL of precooled methanol were added, and the mixture was vortexed again before being ultrasonicated in a low-temperature water bath for 20 minutes. After incubation at room temperature for 30 minutes, the samples were centrifuged at 14000 g and 10°C for 15 minutes. The upper organic phase was collected, dried under nitrogen, and reconstituted in 200 μL of a 90% isopropanol or acetonitrile solution. A 90 μL aliquot of the reconstituted solution was centrifuged under the same conditions, and the supernatant was used for mass spectrometry analysis.

Chromatographic Conditions

The samples were analyzed using the UHPLC Nexera LC-30A system, featuring a C18 column maintained at a temperature of 45°C, with a flow rate of 300 μL/min. The mobile phase comprised Solution A (60% acetonitrile and 40% water) and Solution B (10% acetonitrile and 90% isopropanol). The gradient elution program was structured as follows: for the first 2 minutes, 30% of Solution B was utilized; from 2 to 25 minutes, the proportion of Solution B was gradually increased from 30% to 100%; and from 25 to 35 minutes, it was returned to 30% of Solution B. The samples were stored in an autosampler at a temperature of 10°C. To minimize fluctuations in the signal, the samples were analyzed in a random sequence.

Experimental Conditions for Mass Spectrometry Analysis

Detection was performed in both positive and negative ion modes using electrospray ionization. Following separation via UHPLC, the samples underwent mass spectrometry analysis with a Q Exactive series mass spectrometer (Thermo Scientific™).

Molecular Analysis of Experiment Rat PFC Tissue

RT-qPCR

Total RNA was extracted from the prefrontal cortex of rats using the EZBioscience® Tissue RNA Purification Kit (EZBioscience, Roseville, MN, USA). The concentration and purity of the isolated RNA were assessed using a NanoDrop™ Lite spectrophotometer (Thermo Fisher Scientific, Waltham, MA, USA). An optical density (OD) ratio (OD260/OD280) between 1.8 and 2.0 indicated high-quality RNA. Next, 1 μg of total RNA was reverse transcribed into cDNA using the Reverse Transcription Kit (EZBioscience). Quantitative real-time PCR (RT-qPCR) amplification was performed with the Bestar® Sybr Green qPCR Master Mix (DBI Bioscience, Shanghai, China). The primer sequences are provided in Table 1. RT-qPCR reactions were conducted on the CFX96™ Real-Time Touch System (Bio-Rad Laboratories, Hercules, CA, USA), with glyceraldehyde 3-phosphate dehydrogenase (*Gapdh*) as the internal reference gene. Each PCR reaction consisted of 1 μL of cDNA in a final volume of 10 μL. The thermal cycling conditions included initial denaturation at 95°C for 2 minutes, followed by 40 cycles of denaturation at 95°C for 10 seconds, annealing at 58°C for 30 seconds, and extension at 72°C for 30 seconds. The specificity of the RT-qPCR products was confirmed through

Table 1 Primer Sequence for RT-qPCR Analysis

Gene	Forward Primer 5′-3′	Reverse Primer 5′-3′
Gapdh	ATTCTTCCACCTTTGATGCTGG	TGCTGTAGCCATATTCATTGTCA
Sphk1	GGGGAGATTCGTTTCACGGT	ACGAGGTATGTGTTGGCAGG
Sphk2	GTTGCTCAACTGCTCGCTTC	GAATCCCCAGGCAACTGACA
Cerk	TGGCCGATGGCATAGAATGG	GCTTCGGTCTTGAAGTCAGGT
Cers1	CATCGCCTCTTCCTATGCG	CACCCCTGGCCTTGAAGTAG
Smpd1	ATGCCTTTGGGTGGAGGAAC	CTGGCACACATTTAGTGGCG
Hexa	GGCCCCAGTACATCCAAACC	GAATGTTCTTCCCCAACGGC
Sgms1	GCTGGCCTTTCTTTACGCAC	CAGGTACAGCGTGCCAACTA

melting curve analysis. Relative expression levels were calculated using the $2^{-\Delta\Delta CT}$ method. All experiments were repeated at least three times to ensure reproducibility.

Western Blotting

Proteins were extracted from the prefrontal cortex of rats using RIPA buffer supplemented with protease inhibitors. Protein concentrations were quantified using the BCA method. The proteins were denatured at 95°C for 5 minutes. A total of 30 μg of protein was loaded onto and separated on 10% SDS-PAGE gels, which were subsequently transferred to polyvinylidene fluoride (PVDF) membranes. The membranes were blocked with 5% skimmed milk powder for 1 hour at room temperature. Primary antibodies were incubated overnight at 4°C in the following concentrations: GAPDH (1:10,000; Proteintech, China), β-Tubulin (1:4000; Proteintech), CERK (1:1000; ABclonal, China), CERS1 (1:1000; Huamei Bio, China), SMPD1 (1:1500; ABclonal), SGMS1 (1:1000; ABclonal), HEXA (1:700; ABclonal), SPHK1 (1:1000; Proteintech), SPHK2 (1:1000; Wanlei Bio), DBH (1:500; ABclonal), DRD1 (1:700; Proteintech), MAOA (1:1000; Proteintech), and TH (1:2000; Proteintech). After washing the membranes three times with TBST for 10 minutes each, they were incubated with horseradish peroxidase-conjugated secondary antibodies (1:5000; Proteintech) at room temperature for 1 hour. Following the final wash, bands were visualized using an enhanced chemiluminescence reagent (FDbio-Dura ECL, China) and captured using the ChemiDoc™MP imaging system (Bio-Rad Laboratories). Protein quantification was performed using ImageJ software (version 1.52). All experiments were repeated at least three times.

ELISA

S1P levels in the prefrontal cortex of rats were measured using an S1P ELISA Kit from MeiMIAN (Salt Lake City, UT, China). All experimental procedures were strictly conducted following the manufacturer's protocol. A standard curve was created based on the protein content of the samples (nmol/L) to determine the concentration of each sample. The concentration of S1P in the PFC tissues was reported in moles.

Relative Quantitative Analysis of Immunofluorescence

Paraffin from rat prefrontal cortex tissue was dewaxed, subjected to antigen retrieval, and blocked with bovine serum albumin. The tissue sections were incubated overnight at 4°C with primary antibodies: SPHK1 (1:200; Proteintech, China) and SPHK2 (1:200; Wanlei Bio, China). Following this incubation, the sections were treated with secondary antibodies corresponding to the primary antibodies for 1 hour. The cell nuclei were counterstained with DAPI, and the sections were mounted. Scanning of the sections was performed using a Nikon confocal microscope (model A1 (HD25)), and quantitative analysis was conducted using ImageJ software (version 1.52). This experiment was repeated at least three times to ensure reliability.

Animal Intervention

SKI II is a synthetic sphingosine kinase (SPHK) inhibitor that specifically targets SPHK1 and SPHK2. When administered intraperitoneally, it effectively reduces the levels of S1P in the brain and irreversibly inhibits SPHK1.[35] This mechanism has potential therapeutic applications in the treatment of cancer and neurodegenerative diseases.[36] In this

study, 4-week-old male SHR were randomly assigned to either the SKI II intervention group (SHR + SKI II) or a control SHR group, while age-matched WKY rats served as further controls. Each group consisted of 5–7 rats. The SHR + SKI II group received intraperitoneal injections of SKI II at a dose of 15 mg/kg. The diluent composition used was 2% DMSO, 40% PEG300, 5% Tween-80, and 53% saline. Treatments were administered once every other day for a total of 9 injections.

Behavior Analysis

All experiments were carried out in a controlled and quiet environment. One hour before each trial, the animals were acclimated to the experimental setting by being placed in the behavioral laboratory. To account for the animals' circadian rhythms, all trials were conducted within a consistent time window. After each trial, the animals were promptly returned to their respective breeding cages. The experimental apparatus was thoroughly disinfected with a 75% ethanol solution to eliminate any residual odors. Trials resumed only after the smell of the alcohol had completely dissipated.

Open Field Test

The open field test (OFT) is designed to evaluate rodents' spontaneous motor activity and exploration behavior in a novel environment.[37] The experiment utilized a black organic glass cube measuring 100 cm×100 cm×60 cm, with the floor divided into 16 squares (4×4) using Visu Track software. The central area is defined by the four middle squares and has a diameter of 50 cm. For the test, animals were taken from their breeding cage and placed in the lower right corner of the open field, facing away from the experimenter, for a 5-minute observation period. Key parameters measured during the test include total distance traveled, time spent in the central area, and the number of rearing events.

Elevated Plus Maze Experiment

The anxiety-like behavior of rodents was assessed using the elevated plus maze (EPM) test.[38] The apparatus consists of two open arms and two enclosed arms arranged in a cross shape, with a central area at the intersection elevated 60 cm above the ground. The experiment consisted of two phases: habituation and testing. During the habituation phase, experimental animals were placed in the testing apparatus for a 5-minute adaptation period. Following a 24-hour interval, behavioral testing was conducted in the same apparatus. During the experiment, rats were placed in the central area facing one of the open arms, with their backs toward the experimenter. They were allowed to explore the maze freely for 5 minutes. The total distance traveled, the number of entries into the open arms, and the time spent in the open arms were recorded.

Y-Maze Experiment

The Y-maze spontaneous alternation test is a behavioral procedure that utilizes animals' natural exploratory instincts and is commonly used to evaluate short-term spatial working memory.[39] The apparatus consists of a Y-shaped maze made of black plastic, with three arms, each measuring 40 cm in length, 10 cm in width, and 25 cm in height, arranged at 120° angles. The experiment consisted of two phases: habituation and testing. During the habituation phase, experimental animals were placed in the testing apparatus for a 5-minute adaptation period. Following a 24-hour interval, behavioral testing was conducted in the same apparatus. During the experiment, a mouse is placed at the end of one arm and allowed to explore the maze freely for 5 minutes. A camera system records the total number of entries into each arm as well as the order of visits. An alternation event occurs when the mouse enters all three arms consecutively without immediately re-entering the same arm. The alternation percentage is calculated using the formula: (number of alternations / (total number of entries - 2)) * 100%.

Marble Burial Test

The marble burial test (MBT) is a well-established method used to assess impulsive behavior in rodents.[40] In this experiment, a standard cage measuring 40 cm×25 cm×20 cm is lined with a 5 cm thick layer of wood shavings. Within the cage, 24 standardized glass marbles, each approximately 1 cm in diameter, are arranged systematically in a 4×6 grid. At the start of the experiment, a single rat is placed in one corner of the cage. The observer then discreetly exits the room, allowing the rat to explore the cage freely for 30 minutes. After this period, the rat is carefully removed without

disturbing the marbles, and the number of buried marbles is recorded. A marble is considered buried if wood shavings cover more than two-thirds of its volume.

Data Processing and Statistical Analysis

Statistical analysis of the experimental data was performed using GraphPad Prism 9 software. The results of each group of experimental data were expressed in the form of mean ± standard error (Mean ± SEM). Student's *t*-test was used to compare the two groups. One-way analysis of variance (ANOVA) was used for comparison among groups with more than two groups. $p < 0.05$ criterion was considered statistically significant (*$p < 0.05$, **$p < 0.01$, ***$p < 0.001$), and ns indicates $p \geq 0.05$.

Results

Identification and Differential Analysis of Lipid Metabolites

Using high-resolution mass spectrometry in both positive and negative ion modes, we identified 42 lipid subclasses and 1633 lipid molecules (Figure 1A). Glycerophospholipids and sphingolipids constituted over 70% of the identified lipids, representing core lipidomic features (Figure 1B). Circular visualization of lipid subclass relative abundance across groups (Figure 1C) and ANOVA analysis revealed no significant differences in total lipid content, suggesting metabolic phenotype alterations are likely driven by specific lipid subclasses or molecules rather than global lipid level changes. Principal component analysis (PCA) of metabolic profiles demonstrated limited intergroup separation, with the first principal component (PC1) accounting for 24.95% of the variance and PC2 explaining 12.11% (Figure 1D). The overlapping distribution pattern indicated relatively low effect sizes between groups in global lipid metabolic profiles. Notably, orthogonal partial least squares discriminant analysis (OPLS-DA) effectively segregated the four experimental groups along the T[1] axis (Figure 1E), confirming characteristic lipid metabolic dysregulation in the ADHD model.

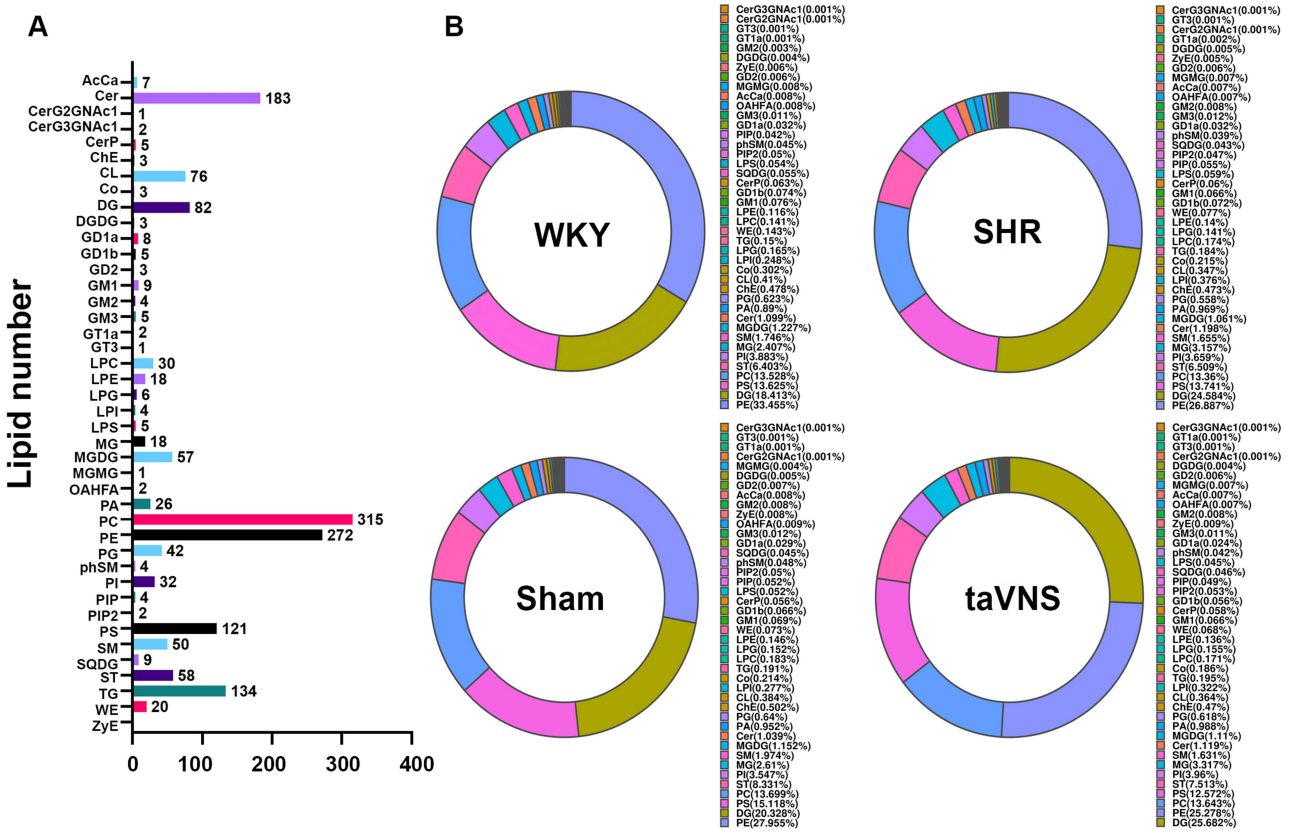

Figure 1 Continued.

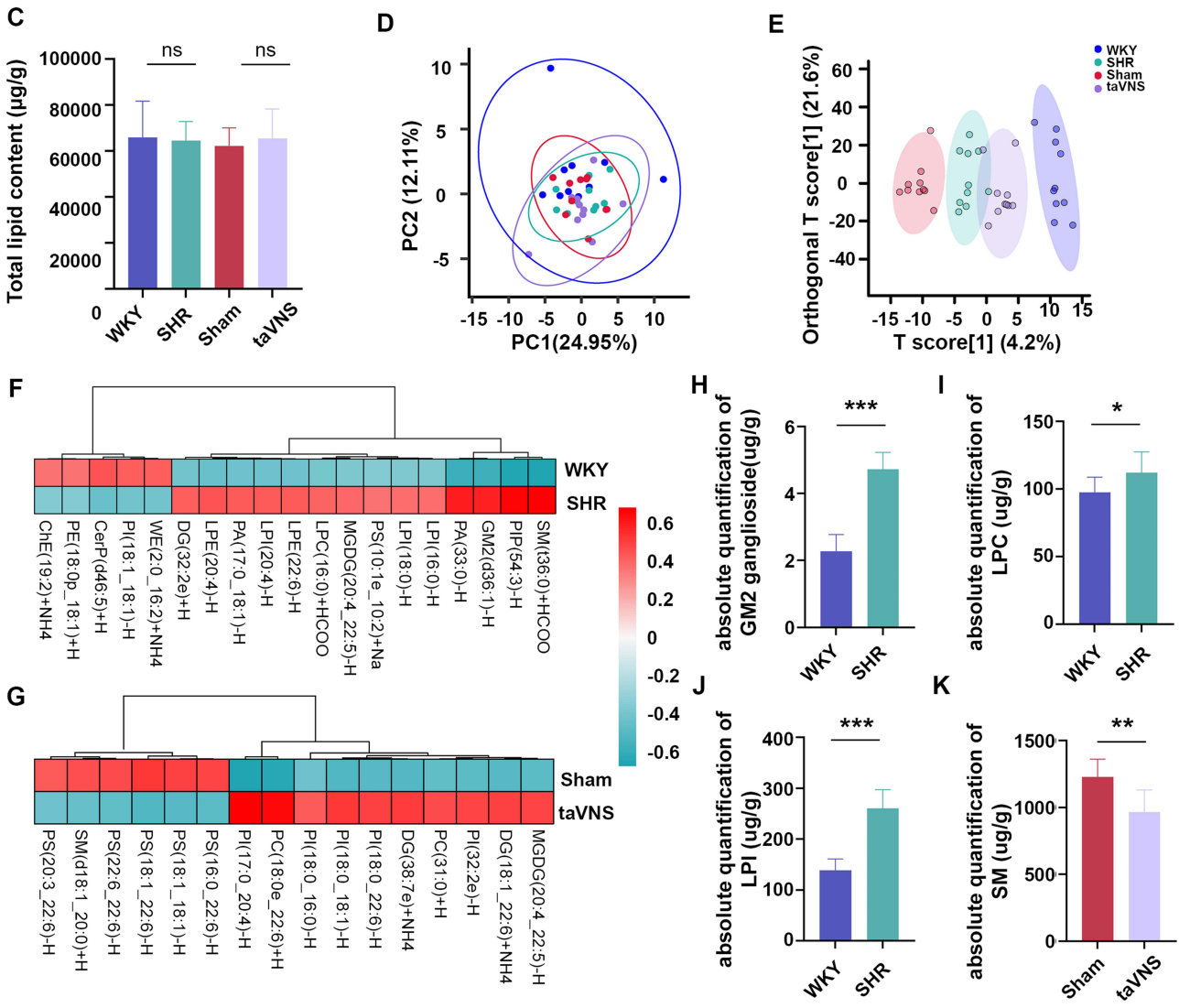

Figure 1 Lipidomics analysis (**A**) Number of 42 lipid subclasses and 1633 lipid molecules identified. (**B**) Ring diagram of lipid subclass composition. (**C**) Total lipid content. (**D**) PCA score plot. Each dot represents an individual sample. The distribution of samples reflects their similarities and differences in lipid metabolic profiles: closer proximity indicates greater similarity in lipid metabolite types and levels, while larger distances correspond to more significant differences in overall metabolic levels. (**E**) OPLS-DA score plot. (**F**) Heatmap of the mean standardized amount of different lipid molecules in the WKY group versus the SHR group. Red indicates significant upregulation of lipid molecules, and green indicates significant downregulation; the color gradient reflects the magnitude of their relative changes. (**G**) Heatmap of the average standardized amount of difference lipid molecules in the Sham group versus the taVNS group. Color coding follows the same convention as in (**F**). (**H**) GM2 lipid content. (**I**) LPC lipid content. (**J**) LPI lipid content. (**K**) SM lipid content. Each value represents the mean ± standard deviation of at least three independent experiments. *$p < 0.05$, **$p < 0.01$, ***$p < 0.001$.
Abbreviation: ns, not statistically significant.

Through OPLS-DA modeling (VIP > 1 and $p < 0.05$), we identified 19 differentially expressed lipids between WKY and SHR groups (Figure 1F), and 16 differential lipids between Sham and taVNS groups (Figure 1G). The standardized heatmap, generated following mean-centering normalization, reveals that differential lipid molecules across groups exhibit distinct upregulated or downregulated patterns (Figure 1H–J). Absolute quantification demonstrated significant elevations of ganglioside GM2, lysophosphatidylcholines (LPC), and lysophosphatidylinositols (LPI) in SHR versus WKY controls. Conversely, taVNS intervention markedly reduced sphingomyelin (SM) levels compared to the Sham group (Figure 1K).

https://doi.org/10.2147/NDT.S530564

Sphingolipid Metabolic Enzyme Expression at mRNA and Protein Levels

We first illustrated the distribution and functional roles of key enzymes in the sphingolipid metabolic pathway by a schematic diagram (Figure 2). Subsequent analyses quantified mRNA and protein expression levels of these enzymes in the prefrontal cortex. SHR rats exhibited significant upregulation of *Sphk1* and *Sphk2* mRNA compared to WKY controls (Figure 3A and B). While taVNS intervention reduced *Sphk2* expression versus the Sham group (Figure 3B), it did not alter *Sphk1* levels (Figure 3A). *Cers1* and *Cerk* mRNA were downregulated in SHR rats (Figure 3C and D), with no rescue effect observed after taVNS treatment. taVNS significantly upregulated *Hexa* and *Smpd1* mRNA compared to the Sham group (Figure 3E and F), though no intergroup differences were detected between WKY and SHR. *Sgms1* mRNA showed no significant variation across all groups (Figure 3G). SPHK1 and SPHK2 protein levels were elevated in SHR rats versus WKY controls (Figure 4A–C), aligning with mRNA trends. However, taVNS did not significantly modulate these proteins. No intergroup differences were detected for CERS1, CERK, HEXA, SMPD1, or SGMS1 proteins (Figure 4D–J). These findings indicate selective dysregulation of SPHK isoforms at both transcriptional and translational levels in the SHR prefrontal cortex, suggesting sustained activation of the SPHK-S1P signaling axis may contribute to ADHD pathophysiology.

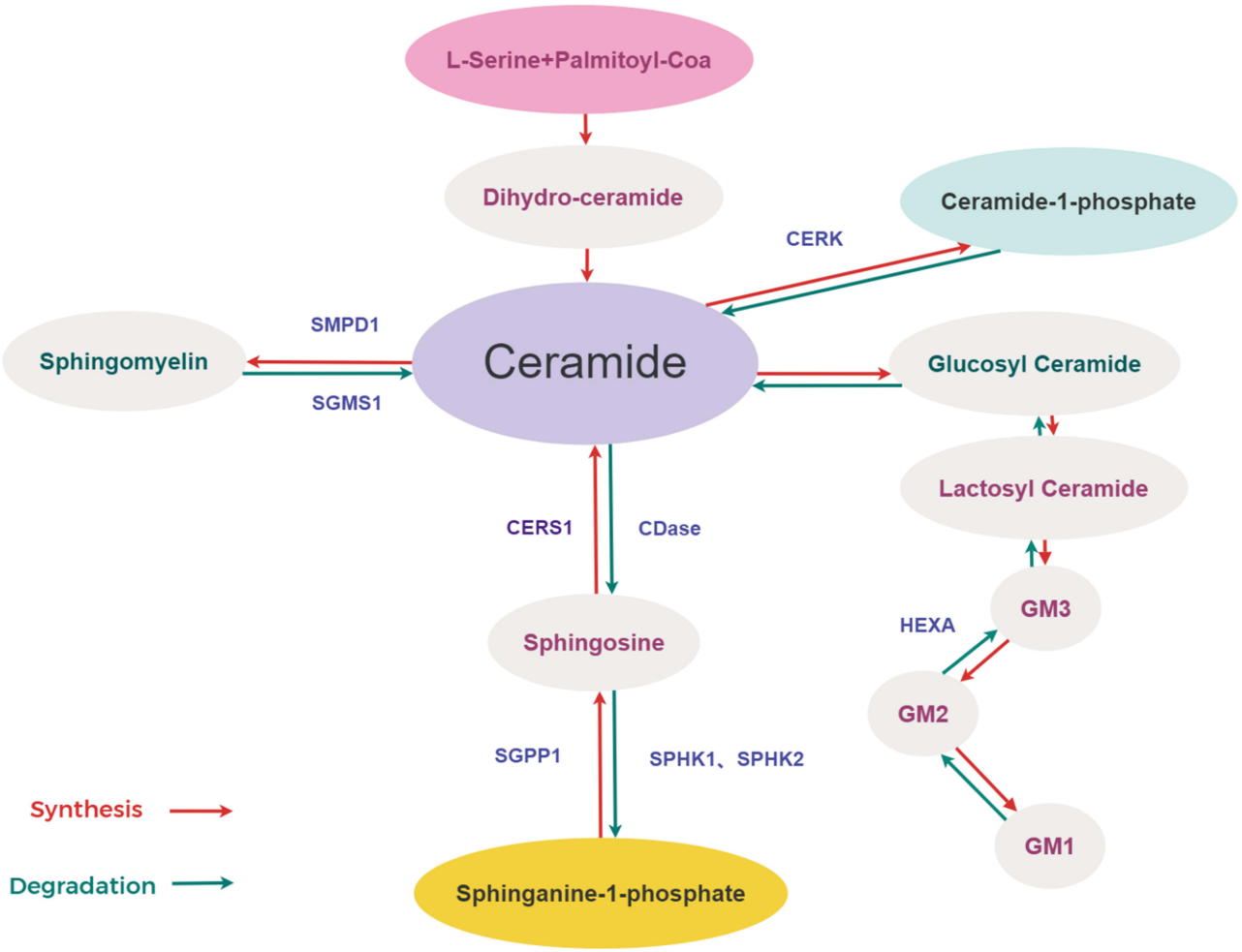

Figure 2 Schematic Diagram of Sphingolipid Metabolism Red arrows indicate synthesis pathways and green arrows denote degradation pathways.
Abbreviations: SMPD1, Sphingomyelin phosphodiesterase 1; SGMS1, Sphingomyelin synthase 1; CERK, Ceramide kinase; CERS1, Ceramide synthase 1; CDase, Ceramidase; SGPP1, Sphingosine-1-phosphate phosphatase 1; SPHK1, Sphingosine kinase 1; SPHK2, Sphingosine kinase 2; HEXA, Hexosaminidase A.

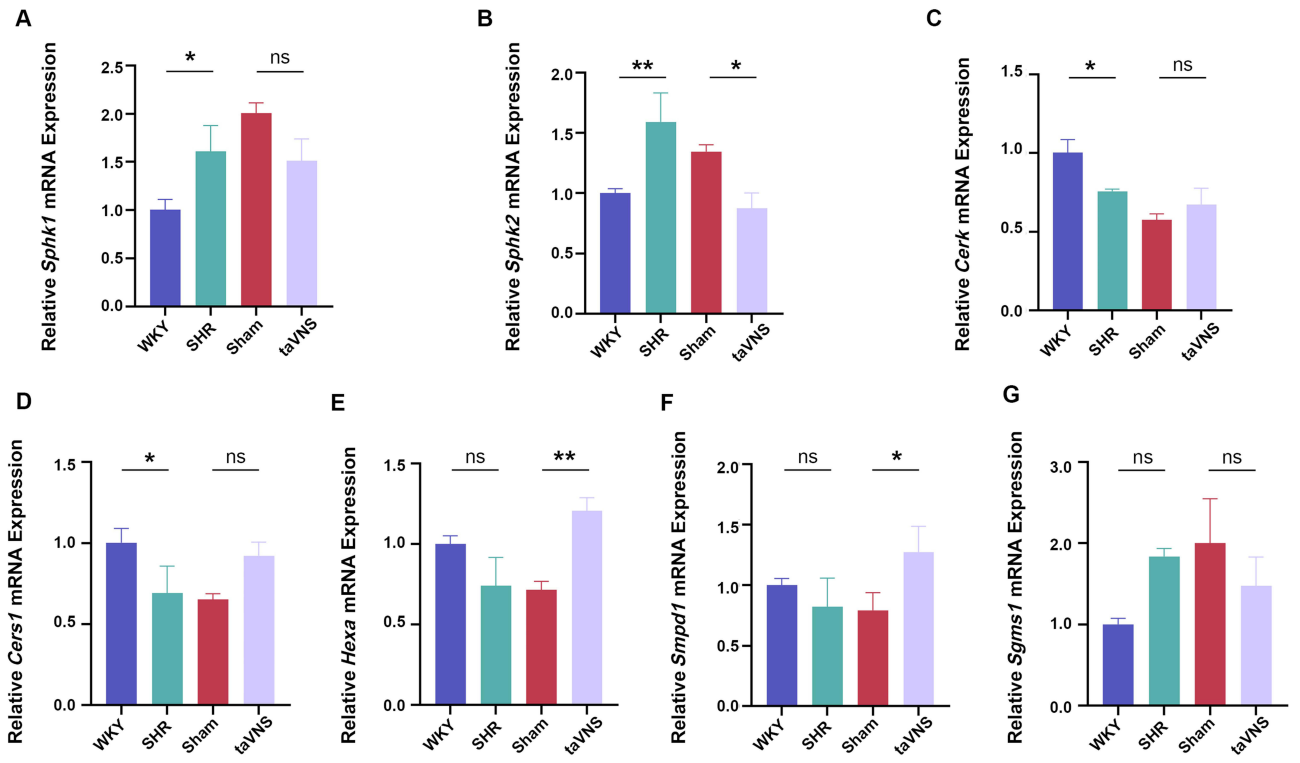

Figure 3 mRNA expression analysis of sphingolipid metabolism-related enzymes in the PFC of rats (**A**) Relative expression levels of *Sphk1* mRNA. (**B**) Relative expression levels of *Sphk2* mRNA. (**C**) Relative expression levels of *Cers1* mRNA. (**D**) Relative expression levels of *Cerk* mRNA. (**E**) Relative expression levels of *Smpd1* mRNA. (**F**) Relative expression levels of *Hexa* mRNA. (**G**) Relative expression levels of *Sgms1* mRNA. Each value represents the mean ± standard deviation of at least three independent experiments. *$p < 0.05$, **$p < 0.01$.
Abbreviation: ns, not statistically significant.

Altered SPHK Expression and S1P Accumulation in the Prefrontal Cortex of SHR Rats

The aforementioned findings suggested potential dysregulation of SPHK protein expression in the prefrontal cortex of SHR rats. To validate this hypothesis, we performed immunofluorescence analysis targeting SPHK1 and SPHK2. Results demonstrated marked elevation of both SPHK1 and SPHK2 protein levels in SHR rats compared to WKY controls, whereas no significant differences were observed between taVNS and Sham groups (Figures 5, 6 and 7A, B).

Given the critical role of SPHK1/2 in catalyzing sphingosine phosphorylation to generate S1P, we further quantified S1P concentrations via ELISA. The SHR rats exhibited significantly higher prefrontal cortical S1P levels than WKY rats, with taVNS intervention showing no modulatory effect compared to the Sham group (Figure 7C). This multi-level validation strongly implicates SPHK-S1P pathway hyperactivity as a potential pathological mechanism underlying ADHD. Furthermore, the absence of taVNS-mediated modulation on this pathway suggests its therapeutic effects may involve alternative signaling axes.

SKI II Intervention Attenuates Hyperactivity and Impulsivity in SHR Rats

In OFT, Compared to the WKY controls, SHR rats displayed significantly increased total movement distance (Figure 8A and B) and rearing frequency (Figure 8C), indicative of locomotor hyperactivity and disinhibited exploratory behavior. SKI II intervention markedly reduced both total ambulatory distance (Figure 8B) and rearing events (Figure 8C). Paradoxically, SHR rats exhibited prolonged central zone occupancy compared to WKY controls (Figure 8D), which normalized toward WKY levels following SKI II treatment, potentially attributable to reduced locomotor output.

MBT assays revealed compulsive behavior in SHR rats, with higher burying rates compared to WKY control. SKI II administration decreased SHR burying activity by demonstrating improved impulse control (Figure 8E).

EPM analyses showed SHR rats maintained greater total locomotion than the WKY control, which SKI II suppressed. Intriguingly, despite their hyperactivity, SHR rats displayed longer open-arm dwell time than the WKY control. SKI II

https://doi.org/10.2147/NDT.S530564

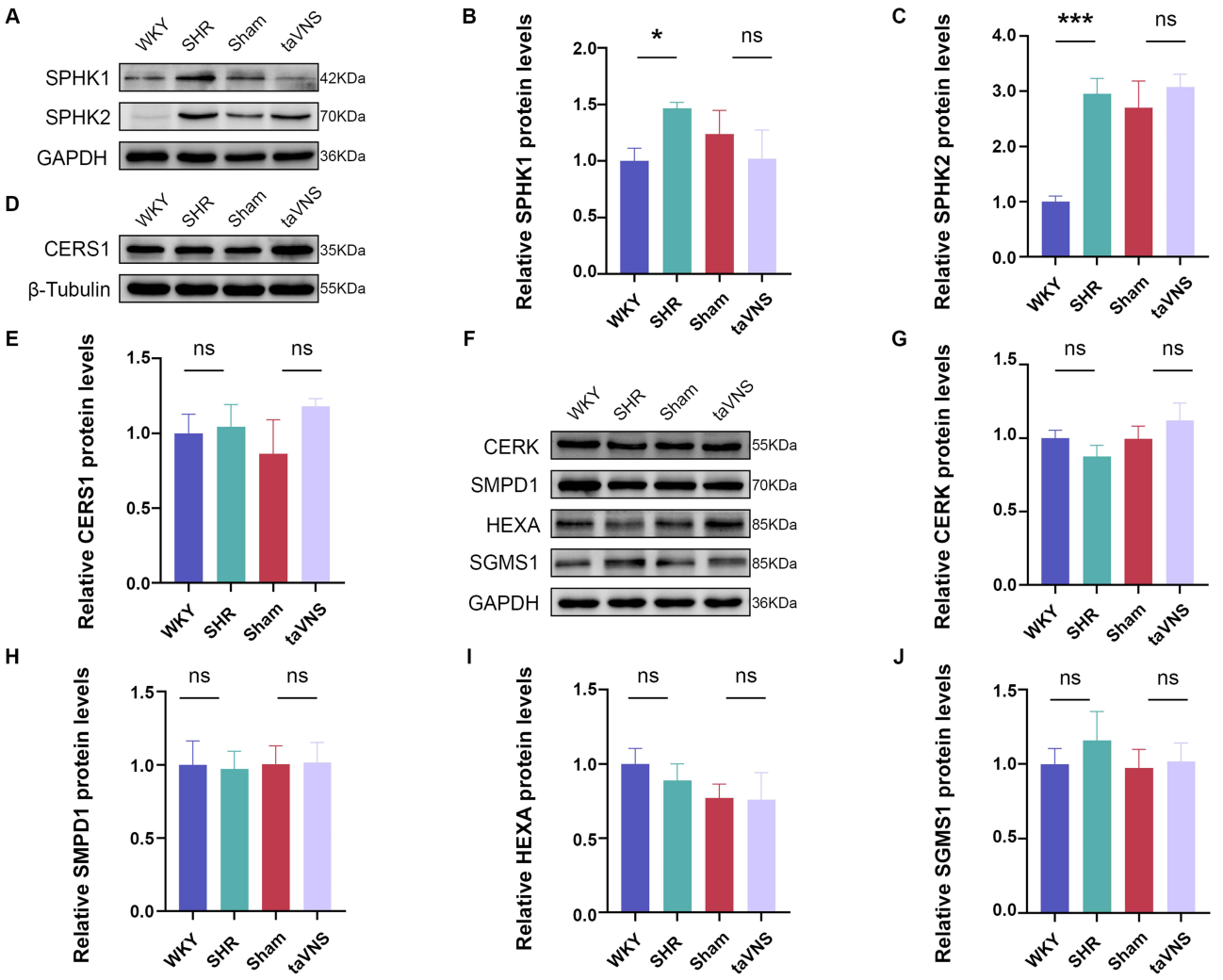

Figure 4 Protein expression analysis of sphingolipid metabolism-related enzymes in the PFC (**A**) Representative Western blotting bands for the ratio of SPHK1/GAPDH, SPHK2/GAPDH. (**B**) Relative protein levels of SPHK1. (**C**) Relative protein levels of SPHK2. (**D**) Representative Western blotting bands for the ratio of CERS1/β-Tubulin. (**E**) Relative protein levels of CERS1. (**F**) Representative Western blotting bands for the ratio of CERK/GAPDH, SMPD1/GAPDH, SGMS1/GAPDH. (**G**) Relative protein levels of CERK. (**H**) Relative protein levels of SMPD1. (**I**) Relative protein levels of HEXA. (**J**) Relative protein levels of SGMS1. Each value represents the mean ± standard deviation of at least three independent experiments. * $p < 0.05$, *** $p < 0.001$.
Abbreviation: ns, not statistically significant.

further enhanced this parameter while increasing open-arm entries, suggesting specific anxiolytic effects beyond locomotor modulation (Figure 8F–H).

The Y-maze experiment assessed the spatial working memory ability. In Y-maze assessments, SHR rats showed a higher number of alternations compared to the WKY control, likely reflecting hyperactivity-driven artifacts rather than cognitive enhancement (Figure 8J). SKI II restored alternation frequency to WKY levels while reducing total movement distance, consistent with OFT and EPM findings (Figure 8I).

Collectively, these behavioral improvements confirm that SPHK-S1P pathway inhibition alleviates ADHD-relevant phenotypes through mechanisms involving both motor activity regulation and impulsivity modulation.

SKI II Intervention Downregulates SPHK-S1P Signaling in the Prefrontal Cortex of SHR Rats

To elucidate the molecular mechanism underlying SKI II intervention, we analyzed SPHK1 and SPHK2 expression dynamics in the prefrontal cortex across experimental groups. RT-qPCR revealed a significant reduction in *Sphk1* mRNA

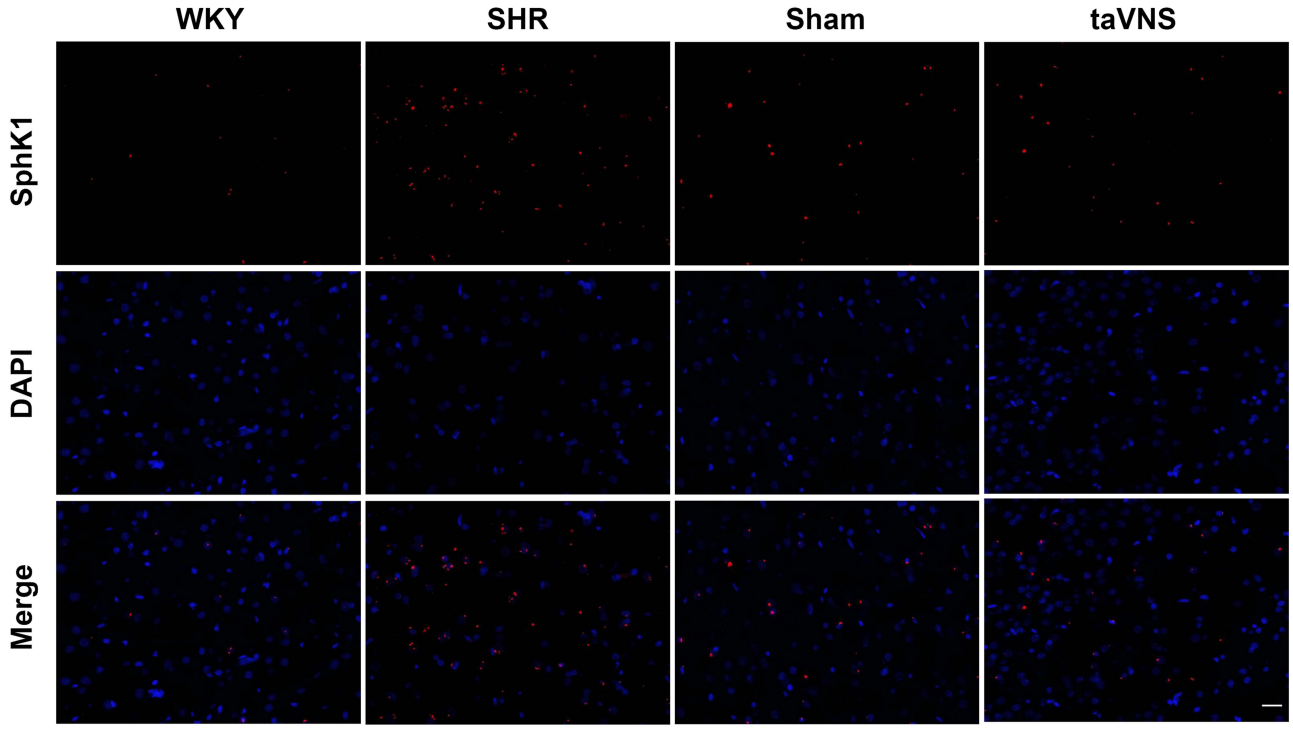

Figure 5 Representative immunofluorescence images of SPHK1 expression in rat PFC tissue sections. Scale bar = 50 μm. SPHK1 (red); DAPI nuclear counterstain (blue).

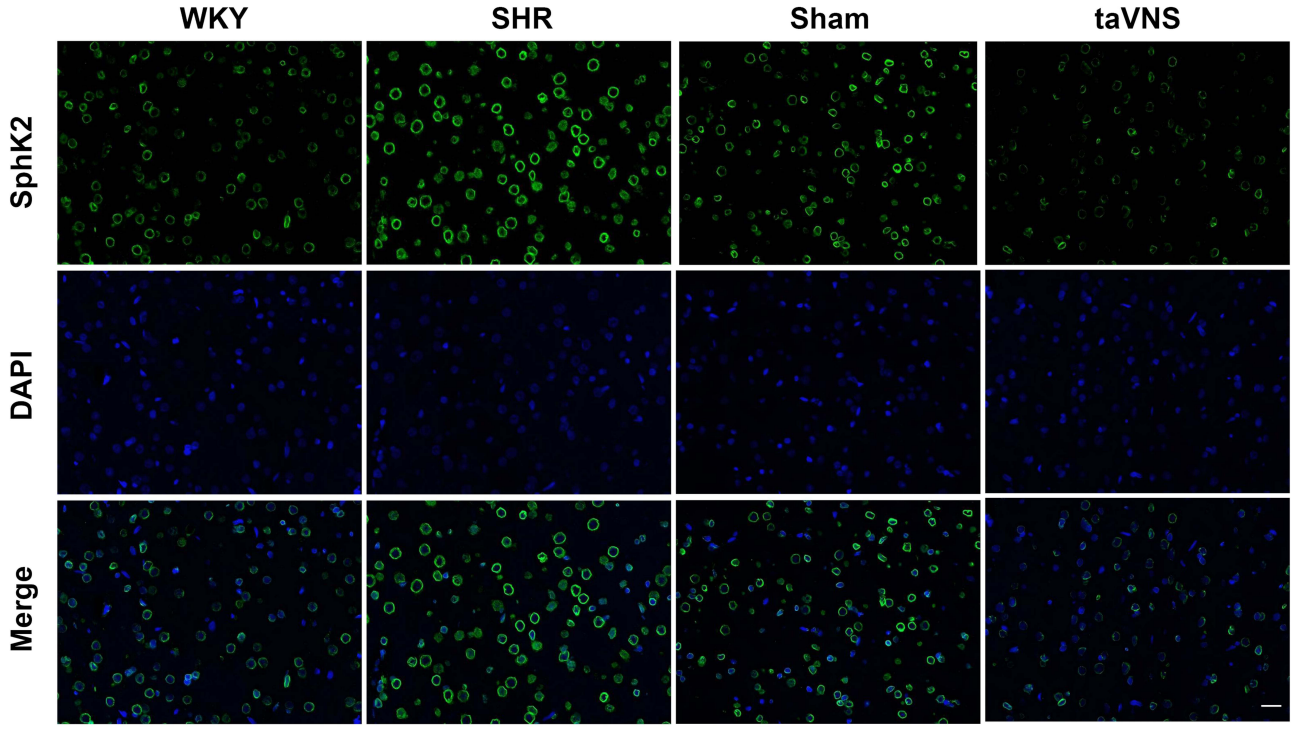

Figure 6 Representative immunofluorescence images of SPHK2 expression in rat PFC tissue sections. Scale bar = 50 μm. SPHK2 (green); DAPI nuclear counterstain (blue).

levels in SKI II treated SHR rats compared to untreated SHR rats (Figure 9A), while *Sphk2* mRNA showed a non-significant downward trend (Figure 9B). Western blot analysis confirmed parallel suppression at the protein level, with SKI II treatment markedly decreasing both SPHK1 (Figure 9C and D) and SPHK2 (Figure 9C and E) expression. ELISA

https://doi.org/10.2147/NDT.S530564

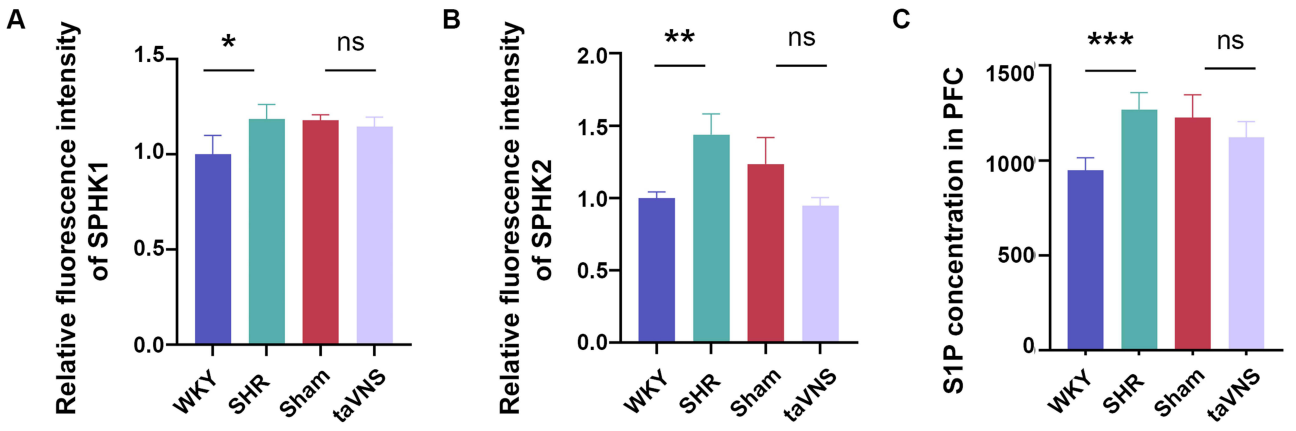

Figure 7 Expression of SPHK and S1P content in PFC tissue sections (**A**) Relative fluorescence intensity of SPHK1. (**B**) Relative fluorescence intensity of SPHK2. (**C**) S1P levels in the PFC were measured by ELISA. Each value represents the mean ± standard deviation of at least three independent experiments. *$p < 0.05$, **$p < 0.01$, ***$p < 0.001$.
Abbreviation: ns, not statistically significant.

quantification further demonstrated a reduction in prefrontal cortical S1P content following SKI II intervention relative to untreated SHR rats (Figure 9F). These multi-omics findings establish that SKI II exerts its therapeutic effects by dual inhibition of SPHK1/SPHK2 expression, thereby attenuating S1P biosynthesis in the ADHD model.

SKI II Modulates Dopaminergic Protein Expression in the Prefrontal Cortex of SHR Rats

We systematically evaluated molecular alterations in the dopaminergic system using Western blot analysis, focusing on dopamine β-hydroxylase (DBH), tyrosine hydroxylase (TH), dopamine D1 receptor (DRD1), and monoamine oxidase A (MAOA). SHR rats exhibited significantly reduced DBH protein levels compared to WKY controls, which were restored to baseline by SKI II intervention (Figure 9G and H). TH and DRD1 showed downward trends in SHR rats, but SKI II treatment failed to reverse these alterations (Figure 9G). MAOA protein abundance remained unchanged across all groups (Figure 9G). These results demonstrate that SKI II specifically rectifies DBH deficiency while exhibiting limited modulatory effects on other dopaminergic markers in the prefrontal cortex of the SHR rats.

Discussion

Sphingolipids, as highly enriched bioactive components in the central nervous system, have been extensively implicated in the pathogenesis of various neurological disorders and neurodegenerative diseases.[41] Our previous integrated bioinformatics analysis of GEO datasets combined with molecular validation revealed significant dysregulation of key sulfatide metabolic pathway genes in ADHD model rats.[42] These differentially expressed genes are functionally interconnected within the sphingolipid metabolic network. Given the established regulatory role of sphingolipid metabolism in myelination,[43] such dysregulation may disrupt sphingolipid homeostasis, thereby interfering with myelination processes and contributing to the neuroconductive dysfunction characteristic of ADHD. The uniqueness of this study, compared with previous research, lies in the following: It is the first to conduct a systematic untargeted lipidomic analysis on prefrontal cortex tissues in an ADHD animal model, clarifying the core role of the SPHK-S1P pathway in ADHD-related sphingolipid metabolic abnormalities. Additionally, it systematically analyzes the activity changes of the SPHK-S1P pathway (including SPHK enzyme activity and S1P levels) in the ADHD animal model, as well as its dose-dependent relationship with behavioral phenotypes such as hyperactivity and impulsivity—an association that has not yet been reported in existing ADHD studies.

The mechanisms underlying lipid metabolic dysregulation in ADHD exhibit remarkable complexity and diversity. Lipids not only govern the localization and functionality of membrane-bound proteins[44] but also modulate neurotransmission by regulating synaptic flux.[45] Recent studies have identified significant alterations in serum lipid and lipoprotein

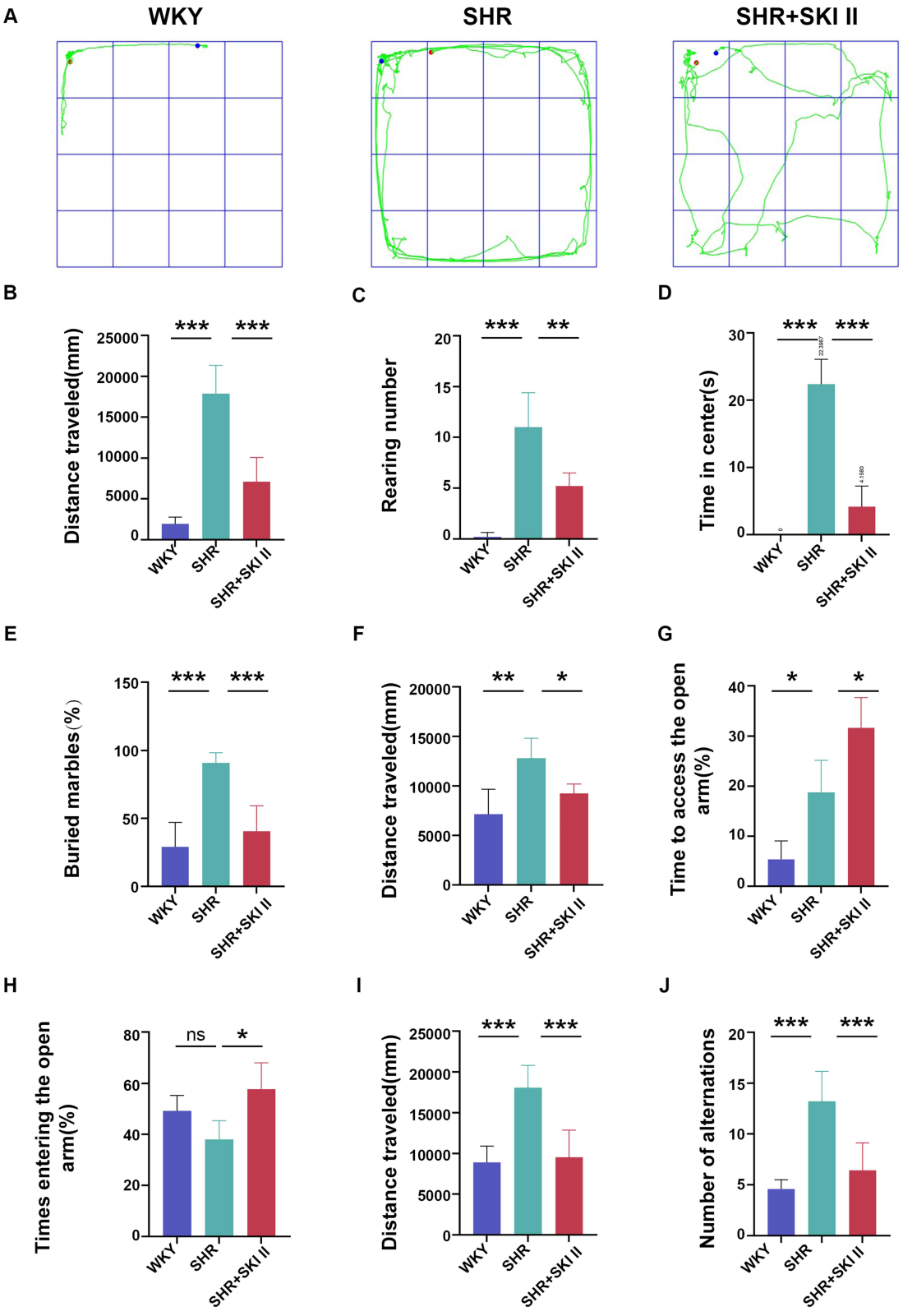

Figure 8 Improvement of ADHD-like behavior in SHR rats by SKI II inhibitors (**A**) Representative map in the OFT field. (**B**) Quantitative plot of the distance traveled in the OFT. (**C**) Number of uprights in the OFT. (**D**) Time spent in the central zone in the OFT. (**E**) Marble burial rate for the marble burial experiment. (**F**) Quantitative plot of distance traveled in the elevated cross maze. (**G**) Percentage of time spent in the open arm of the elevated cross maze. (**H**) Percentage of entries into the open arm of the elevated cross maze. (**I**) Quantitative recording of distance traveled for the Y-maze experiment. (**J**) The number of spontaneous alternations for the Y-maze experiment. Each value represents the mean ± standard deviation of at least three independent experiments. *$p < 0.05$, **$p < 0.01$, ***$p < 0.001$.

Abbreviation: ns, not statistically significant.

https://doi.org/10.2147/NDT.S530564

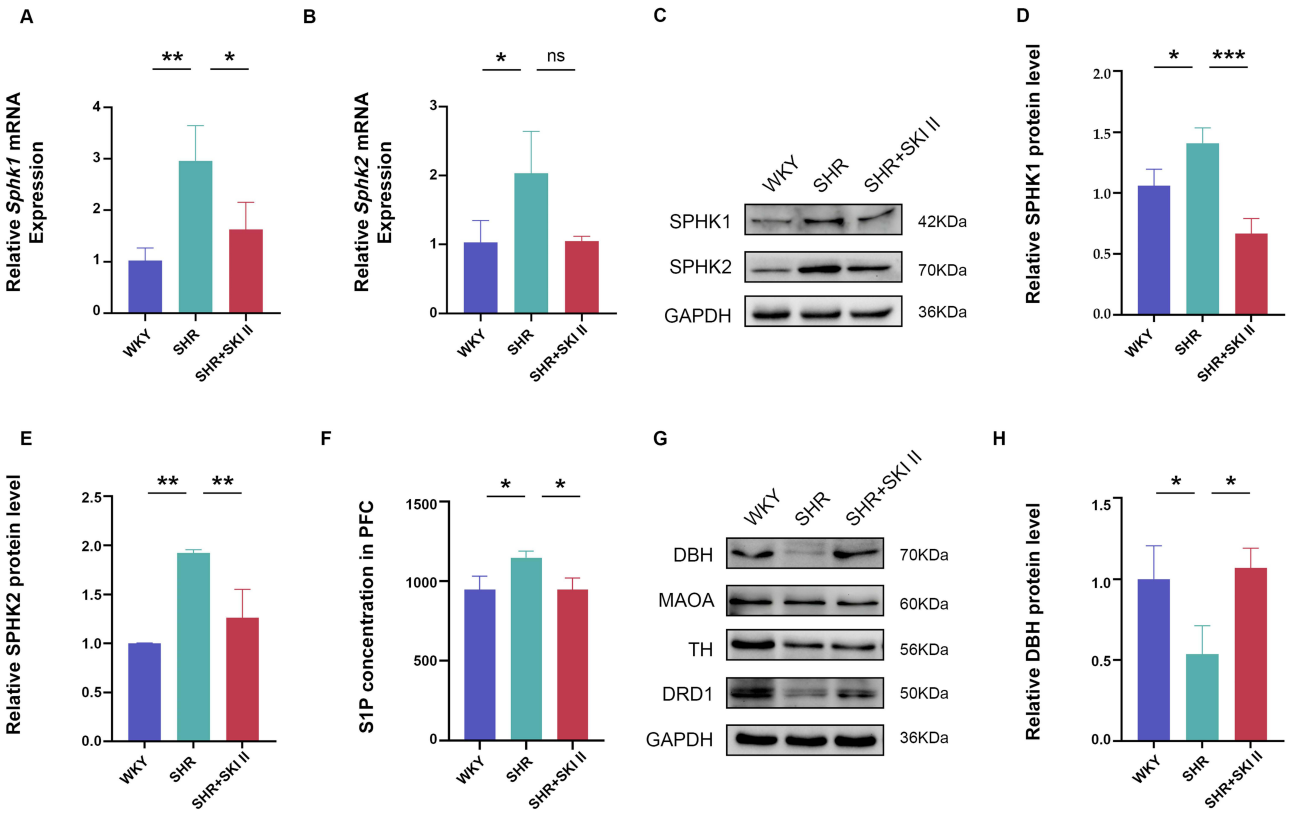

Figure 9 Changes in gene and protein expression following SKI II intervention (**A**) Relative expression levels of *Sphk1* mRNA. (**B**) Relative expression levels of *Sphk2* mRNA. (**C**) Representative Western blot bands showing SPHK1/GAPDH and SPHK2/GAPDH ratios. (**D**) Relative protein levels of SPHK1. (**E**) Relative protein levels of SPHK2. (**F**) S1P levels in the PFC were measured by ELISA. (**G**) Representative Western blot bands showing DBH/GAPDH, MAOA/GAPDH, TH/GAPDH, and DRD1/GAPDH ratios. (**H**) Relative protein levels of DBH. Each value represents the mean ± standard deviation of at least three independent experiments. *$p < 0.05$, **$p < 0.01$, ***$p < 0.001$.

profiles in ADHD patients compared to healthy controls.[17] Our findings further substantiate lipid metabolic abnormalities in the SHR rat model, reinforcing the hypothesis that lipid dyshomeostasis may play a pivotal role in ADHD pathophysiology. While earlier research predominantly focused on the association between fatty acid deficiencies (notably omega-3 polyunsaturated fatty acids) and ADHD symptom exacerbation,[46] emerging evidence has shifted attention toward sphingolipid metabolism. Genetic polymorphisms in sphingolipid-related pathways have demonstrated significant associations with ADHD susceptibility.[21] Recent work by Güleç et al further links altered sphingomyelin and ceramide levels to ADHD symptom severity.[47] As major structural components of central nervous system membranes, sphingolipids are highly enriched in myelin sheaths,[48] and their metabolic imbalance may disrupt neurodevelopmental processes,[19] thereby elevating risks for neurological disorders including ADHD. However, current investigations remain largely descriptive, emphasizing sphingolipid-associated genetic mutations and quantitative lipid alterations. The precise mechanistic pathways through which these changes impair neurodevelopment and manifest as ADHD behavioral phenotypes remain to be fully elucidated.

Emerging evidence indicates reduced serum sphingomyelin and ceramide levels in ADHD patients,[49,50] while plasma concentrations of S1P-d18:1 and S1P-d18:0, exhibit an opposing trend toward elevation.[50] Our findings align with these observations, demonstrating significantly increased S1P levels in the prefrontal cortex of SHR rats. These molecular alterations underscore the intricate balance between ceramide and S1P within sphingolipid metabolism, two metabolites with divergent functional roles in cellular regulation.[22] S1P, a critical mediator of cell survival and autophagy,[51] is synthesized through the catalytic activity of sphingosine kinase isoforms SPHK1 and SPHK2.[52] In this study, we observed elevated enzymatic activity of both SPHK1 and SPHK2 in the prefrontal cortex of SHR rats compared to WKY controls. These findings were corroborated through multi-platform validation encompassing RT-qPCR, Western

blot, and immunofluorescence analyses, with subsequent ELISA quantification further confirming elevated S1P levels in the SHR prefrontal cortex. The SPHK-S1P signaling axis, widely implicated in neurodevelopment, neuronal survival, and neurodegenerative disorders,[13,53] has been linked to cognitive deficits in valproic acid-induced autism models through hippocampal SPHK2/S1P dysregulation.[54] However, no prior studies have directly investigated the association between SPHK-S1P pathway alterations and ADHD pathophysiology. Based on our findings, we hypothesize that prefrontal cortical SPHK-S1P upregulation in SHR rats may mechanistically contribute to ADHD pathogenesis. To test this, we implemented pharmacological intervention using the SPHK inhibitor SKI II, evaluating its dual effects on SPHK-S1P signaling and ADHD-like behavioral phenotypes. This study provides experimental evidence connecting SPHK-S1P pathway hyperactivity to ADHD pathogenesis, offering new perspectives for understanding neurodevelopmental dysregulation in this disorder.

Following SKI II inhibitor intervention, we systematically assessed behavioral alterations in SHR rats alongside SPHK-S1P signaling dynamics and dopaminergic protein expression. Behavioral analyses revealed pronounced ADHD-like phenotypes in untreated SHR rats compared to WKY controls, including hyperactivity[55] and impulsivity (Kantak et al, 2008; Kishikawa et al, 2014), consistent with established ADHD models. Notably, SKI-II intervention ameliorated these behavioral deficits, further supporting the involvement of SPHK-S1P signaling in ADHD pathogenesis.

Reduced dopamine transporter (DAT) levels in ADHD patients may impair dopaminergic signaling, potentially contributing to core behavioral deficits.[56] Neuroimaging studies further demonstrate disrupted dopamine neurotransmission in ADHD brains, which may underlie attention deficits and impulsivity.[57,58] Prefrontal dysfunction, closely linked to hallmark ADHD symptoms such as inattention and hyperactivity,[59] is modulated by the synergistic interplay between norepinephrine and dopamine systems.[60] To investigate the relationship between SPHK-S1P downregulation and behavioral improvements in SHR rats, we analyzed the prefrontal cortex expression of dopaminergic markers, including dopamine β-hydroxylase (DBH), tyrosine hydroxylase (TH), dopamine D1 receptor (DRD1), and monoamine oxidase A (MAOA). DBH, the rate-limiting enzyme converting dopamine to norepinephrine, regulates attentional and behavioral control via catecholamine modulation,[61] with its activity critically influencing ADHD phenotypes.[62] Our results align with prior reports, showing significantly reduced DBH expression in the SHR prefrontal cortex compared to WKY controls.[63] Notably, SKI II intervention reversed this deficit, suggesting SPHK-S1P inhibition may restore DBH-mediated norepinephrine synthesis. While TH, the rate-limiting enzyme in dopamine biosynthesis, exhibited lower expression in SHR rats—consistent with earlier findings[64]—SKI II treatment did not significantly alter TH or DRD1 levels. Similarly, MAOA, which degrades monoamines including dopamine and norepinephrine,[65] showed no intergroup differences. These observations indicate that SPHK-S1P pathway inhibition ameliorates ADHD-like behaviors in SHR rats primarily through DBH upregulation rather than TH, DRD1, or MAOAdependent mechanisms. Collectively, our findings suggest a novel regulatory axis wherein SPHK-S1P signaling selectively modulates DBH expression to influence dopaminergic metabolism, offering a targeted therapeutic strategy for ADHD symptom management. As an initial exploratory study, we focused on validating the relationship between SPHK-S1P signaling and DBH expression, and therefore did not systematically examine other key dopaminergic components like DAT and COMT. This limits our ability to fully characterize the interaction network between SPHK-S1P and dopaminergic function. However, our finding that SPHK-S1P regulates DBH provides a foundation for future studies. We plan to clarify this regulatory network using integrated targeted metabolomics and proteomics, combined with co-expression analysis and in vitro neuronal co-culture models. Given that ADHD pathology involves multi-system crosstalk, subsequent studies should also incorporate integrated analyses with other mechanistic pathways.

Although this study is the first to reveal the aberrant activation of the SPHK-S1P pathway in the ADHD models and its regulatory role in behavioral phenotypes, it remains an exploratory investigation with several limitations that warrant explicit discussion. These shortcomings, however, also provide valuable guidance for refining future research. First, future studies should expand the sample size to n= 10–12 per group and conduct multi-center repeated experiments to enhance the reliability and representativeness of the results. In addition, in the SPHK inhibitor SKI II intervention experiment, although non-specific effects were initially ruled out through dose-dependent effects and the high consistency between behavioral improvement and molecular changes, no independent solvent control group was set up. In subsequent expanded studies, it is necessary to supplement the above control experiments, and combine the comparative

analysis of *SphkPHK* gene knockout models and inhibitory effects to further verify pathway specificity and enhance the rigor of the results. Current findings are entirely derived from animal experiments, and translation to human ADHD pathophysiology requires additional research support. Future plans include establishing links between animal models and human disease through patient-derived induced pluripotent stem cell neuron models and clinical sample analyses. Correlating peripheral blood S1P levels and SPHK activity in ADHD patients with clinical severity scores will enhance translational potential, facilitating the progression of sphingolipid biomarkers toward clinical application. Additionally, untargeted lipidomics data suggest that glycerophospholipid metabolism abnormalities may also contribute to ADHD pathogenesis, but this study did not explore their cross-regulation with the SPHK-S1P pathway in depth. Given the complexity of lipid metabolism cross-regulation, a comprehensive understanding of ADHD pathogenesis will require expanding analyses to encompass multiple metabolic pathways. Finally, the taVNS group included in this study was exploratory, originally designed to test the hypothesis that behavioral regulatory interventions act through sphingolipid metabolism. However, results showed limited impacts of taVNS on sphingolipid metabolism, suggesting its behavioral improvement effects may be mediated via non-lipid-dependent mechanisms. Detailed mechanistic analysis of this group will be reported separately as an independent study, allowing the current work to focus on core findings related to the SPHK-S1P pathway.

These limitations reflect the inherent constraints of exploratory research in terms of mechanistic depth and experimental design completeness. Guided by these insights, we will refine our understanding of the SPHK-S1P pathway's role in ADHD through more systematic experimental designs and multi-dimensional validation, ultimately laying a foundation for its clinical translation.

Institutional Review Board Statement

The animal study protocol was approved by the Institutional Animal Care and Use Committee of Hangzhou Medical University (approval no. 2021-027). All procedures involving the use of animals were conducted in strict accordance with the "Animal Management Regulations of the Ministry of Health of the People's Republic of China" (Document No. 55, 2001) and in accordance with the guidelines of the "Guide for the Care and Use of Laboratory Animals" (National Research Council Committee for the Update of the Guide for the and Use of Laboratory 2011).

Funding

This work was supported by grants from the National Natural Science Foundation of China (grant numbers 82171168 and 81571359) and the Construction Project of Shanghai Key Laboratory of Molecular Imaging (18DZ2260400).

Disclosure

The authors report no conflicts of interest in this work.

References

1. Faraone SV, Asherson P, Banaschewski T, et al. Attention-deficit/hyperactivity disorder. *Nat Rev Dis Primers*. 2015;1(1):15020. doi:10.1038/nrdp.2015.20
2. Thapar A, Cooper M. Attention deficit hyperactivity disorder. *Lancet*. 2016;387(10024):1240–1250. doi:10.1016/S0140-6736(15)00238-X
3. Van meter AR, Sibley MH, Vandana P, et al. The stability and persistence of symptoms in childhood-onset ADHD. *Eur Child Adolesc Psychiatry*. 2024;33(4):1163–1170. doi:10.1007/s00787-023-02235-3
4. Gallo EF, Posner J. Moving towards causality in attention-deficit hyperactivity disorder: overview of neural and genetic mechanisms. *Lancet Psychiatry*. 2016;3(6):555–567. doi:10.1016/S2215-0366(16)00096-1
5. Li Y, Yan X, Li Q, et al. Prevalence and trends in diagnosed ADHD among US children and adolescents, 2017–2022. *JAMA Network Open*. 2023;6(10):e2336872. doi:10.1001/jamanetworkopen.2023.36872
6. Salari N, Ghasemi H, Abdoli N, et al. The global prevalence of ADHD in children and adolescents: a systematic review and meta-analysis. *Ital J Pediatr*. 2023;49(1):48. doi:10.1186/s13052-023-01456-1
7. Cortese S, Song M, Farhat LC, et al. Incidence, prevalence, and global burden of ADHD from 1990 to 2019 across 204 countries: data, with critical re-analysis, from the global burden of disease study. *Mol Psychiatry*. 2023;28(11):4823–4830. doi:10.1038/s41380-023-02228-3
8. Babinski DE. Sex differences in ADHD: review and priorities for future research. *Curr Psychiatry Rep*. 2024;26(4):151–156. doi:10.1007/s11920-024-01492-6
9. Martin J. Why are females less likely to be diagnosed with ADHD in childhood than males? *Lancet Psychiatry*. 2024;11(4):303–310. doi:10.1016/S2215-0366(24)00010-5

10. Pingault JB, Viding E, Galéra C, et al. Genetic and environmental influences on the developmental course of attention-deficit/hyperactivity disorder symptoms from childhood to adolescence. *JAMA Psychiatry*. 2015;72(7):651. doi:10.1001/jamapsychiatry.2015.0469
11. Pang T, Ding N, Zhao Y, Zhao J, Yang L, Chang S. Novel genetic loci of inhibitory control in ADHD and healthy children and genetic correlations with ADHD. *Prog Neuro Psychopharmacol Biol Psychiatry*. 2024;132:110988. doi:10.1016/j.pnpbp.2024.110988
12. Swanson JM, Kinsbourne M, Nigg J, et al. Etiologic subtypes of attention-deficit/hyperactivity disorder: brain imaging, molecular genetic and environmental factors and the dopamine hypothesis. *Neuropsychol Rev*. 2007;17(1):39–59. doi:10.1007/s11065-007-9019-9
13. van Kruining D, Luo Q, van Echten-Deckert G, et al. Sphingolipids as prognostic biomarkers of neurodegeneration, neuroinflammation, and psychiatric diseases and their emerging role in lipidomic investigation methods. *Adv Drug Delivery Rev*. 2020;159:232–244. doi:10.1016/j.addr.2020.04.009
14. Hornemann T. Mini review: lipids in peripheral nerve disorders. *Neurosci lett*. 2021;740:135455. doi:10.1016/j.neulet.2020.135455
15. Zhang J, Liu Q. Cholesterol metabolism and homeostasis in the brain. *Protein Cell*. 2015;6(4):254–264. doi:10.1007/s13238-014-0131-3
16. Hussain G, Wang J, Rasul A, et al. Role of cholesterol and sphingolipids in brain development and neurological diseases. *Lipids Health Dis*. 2019;18(1):26. doi:10.1186/s12944-019-0965-z
17. Ugur C, Uneri OS, Goker Z, Sekmen E, Aydemir H, Solmaz E. The assessment of serum lipid profiles of children with attention deficit hyperactivity disorder. *Psychiatry Res*. 2018;264:231–235. doi:10.1016/j.psychres.2018.04.006
18. Farooqui AA, Horrocks LA, Farooqui T. Glycerophospholipids in brain: their metabolism, incorporation into membranes, functions, and involvement in neurological disorders. *Chem Phys Lipids*. 2000;106(1):1–29. doi:10.1016/s0009-3084(00)00128-6
19. Hannun YA, Obeid LM. Sphingolipids and their metabolism in physiology and disease. *Nat Rev Mol Cell Biol*. 2018;19(3):175–191. doi:10.1038/nrm.2017.107
20. Yoon JH, Seo Y, Jo YS, et al. Brain lipidomics: from functional landscape to clinical significance. *Sci Adv*. 2022;8(37):eadc9317. doi:10.1126/sciadv.adc9317
21. Henriquez-Henriquez M, Acosta MT, Martinez AF, et al. Mutations in sphingolipid metabolism genes are associated with ADHD. *Transl Psychiatry*. 2020;10(1):231. doi:10.1038/s41398-020-00881-8
22. Piccoli M, Cirillo F, Ghiroldi A, et al. Sphingolipids and atherosclerosis: the dual role of ceramide and sphingosine-1-phosphate. *Antioxidants*. 2023;12(1):143. doi:10.3390/antiox12010143
23. Kurek K, Wiesiołek-Kurek P, Piotrowska DM, Łukaszuk B, Chabowski A, Żendzian-piotrowska M. Inhibition of ceramide *De Novo* synthesis with myriocin affects lipid metabolism in the liver of rats with streptozotocin-induced type 1 diabetes. *Biomed Res Int*. 2014;2014:1–10. doi:10.1155/2014/980815
24. Kumar S, Panda SP. Targeting GM2 ganglioside accumulation in dementia: current therapeutic approaches and future directions. *CMM*. 2024;24(11):1329–1345. doi:10.2174/0115665240264547231017110613
25. Su D, Cheng Y, Li S, Dai D, Zhang W, Lv M. Sphk1 mediates neuroinflammation and neuronal injury via TRAF2/NF-κB pathways in activated microglia in cerebral ischemia reperfusion. *J Neuroimmunol*. 2017;305:35–41. doi:10.1016/j.jneuroim.2017.01.015
26. Jiang ZJ, Gong LW. The SphK1/S1P axis regulates synaptic vesicle endocytosis via TRPC5 channels. *J Neurosci*. 2023;43(21):3807–3824. doi:10.1523/JNEUROSCI.1494-22.2023
27. Ginkel C, Hartmann D, Vom Dorp K, et al. Ablation of neuronal ceramide synthase 1 in mice decreases ganglioside levels and expression of myelin-associated glycoprotein in oligodendrocytes. *J Biol Chem*. 2012;287(50):41888–41902. doi:10.1074/jbc.M112.413500
28. Spassieva SD, Ji X, Liu Y, et al. Ectopic expression of ceramide synthase 2 in neurons suppresses neurodegeneration induced by ceramide synthase 1 deficiency. *Proc Natl Acad Sci USA*. 2016;113(21):5928–5933. doi:10.1073/pnas.1522071113
29. Nishino S, Yamashita H, Tamori M, et al. Translocation and activation of sphingosine kinase 1 by ceramide-1-phosphate. *J Cell Biochem*. 2019;120(4):5396–5408. doi:10.1002/jcb.27818
30. Korade Z, Kenworthy AK. Lipid rafts, cholesterol, and the brain. *Neuropharmacology*. 2008;55(8):1265–1273. doi:10.1016/j.neuropharm.2008.02.019
31. Zhi J, Zhang S, Huang M, et al. Transcutaneous auricular vagus nerve stimulation as a potential therapy for attention deficit hyperactivity disorder: modulation of the noradrenergic pathway in the prefrontal lobe. *Front Neurosci*. 2024;18:1494272. doi:10.3389/fnins.2024.1494272
32. Kim D, Yadav D, Song M. An updated review on animal models to study attention-deficit hyperactivity disorder. *Transl Psychiatry*. 2024;14(1):187. doi:10.1038/s41398-024-02893-0
33. Sagvolden T, Russell VA, Aase H, Johansen EB, Farshbaf M. Rodent models of attention-deficit/hyperactivity disorder. *Biol Psychiatry*. 2005;57(11):1239–1247. doi:10.1016/j.biopsych.2005.02.002
34. Bahmani Z, Clark K, Merrikhi Y, et al. Prefrontal contributions to attention and working memory. In: Hodgson T, editor. *Processes of Visuospatial Attention and Working Memory*. Vol. 41. Switzerland: Springer International Publishing; 2019:129–153. doi:10.1007/7854_2018_74
35. Liu H, Zhang CX, Ma Y, He HW, Wang JP, Shao RG. SphK1 inhibitor SKI II inhibits the proliferation of human hepatoma HepG2 cells via the Wnt5A/β-catenin signaling pathway. *Life Sci*. 2016;151:23–29. doi:10.1016/j.lfs.2016.02.098
36. Pyszko JA, Strosznajder JB. Original article The key role of sphingosine kinases in the molecular mechanism of neuronal cell survival and death in an experimental model of Parkinson's disease. *Folia Neuropathol*. 2014;3:260–269. doi:10.5114/fn.2014.45567
37. Archer J. Tests for emotionality in rats and mice: a review. *Anim Behav*. 1973;21:205–235. doi:10.1016/s0003-3472(73)80065-x
38. Knight P, Chellian R, Wilson R, Behnood-Rod A, Panunzio S, Bruijnzeel AW. Sex differences in the elevated plus-maze test and large open field test in adult Wistar rats. *Pharmacol Biochem Behav*. 2021;204:173168. doi:10.1016/j.pbb.2021.173168
39. Kraeuter AK, Guest PC, Sarnyai Z. The Y-Maze for assessment of spatial working and reference memory in mice. In: Guest PC, editor. *Pre-Clinical Models*. New York: Springer New York; 2019:105–111. doi:10.1007/978-1-4939-8994-2_10
40. de Brouwer G, Fick A, Harvey BH, Wolmarans DW. A critical inquiry into marble-burying as a preclinical screening paradigm of relevance for anxiety and obsessive–compulsive disorder: mapping the way forward. *Cogn Affect Behav Neurosci*. 2019;19(1):1–39. doi:10.3758/s13415-018-00653-4
41. Grassi S, Mauri L, Prioni S, et al. Sphingosine 1-phosphate receptors and metabolic enzymes as druggable targets for brain diseases. *Front Pharmacol*. 2019;10:807. doi:10.3389/fphar.2019.00807
42. Xu Y, Wang Y, He B, Yao Y, Cai Q, Wu L. Identification of the shared gene signatures between autism spectrum disorder and epilepsy via bioinformatic analysis. *Comput Math Methods Med*. 2022;2022:1–17. doi:10.1155/2022/9883537

43. Dasgupta S, Ray SK. Ceramide and sphingosine regulation of myelinogenesis: targeting serine palmitoyltransferase using microRNA in multiple sclerosis. *IJMS*. 2019;20(20):5031. doi:10.3390/ijms20205031
44. Weber-Boyvat M. The lipid transporter ORP2 regulates synaptic neurotransmitter release via two distinct mechanisms. *Cell Rep*. 2022;41:111882. doi:10.1016/j.celrep.2022.111882
45. Tsui-Pierchala BA, Encinas M, Milbrandt J, Johnson EM. Lipid rafts in neuronal signaling and function. *Trends Neurosci*. 2002;25(8):412–417. doi:10.1016/S0166-2236(02)02215-4
46. DiNicolantonio JJ, O'Keefe JH. The importance of marine Omega-3s for brain development and the prevention and treatment of behavior, mood, and other brain disorders. *Nutrients*. 2020;12(8):2333. doi:10.3390/nu12082333
47. Güleç A, Türkoğlu S, Kocabaş R. The relationship between sphingomyelin and ceramide levels and soft neurological signs in ADHD. *J Neural Transm*. 2024;132(1):157–168. doi:10.1007/s00702-024-02831-w
48. Mei M, Liu M, Mei Y, Zhao J, Li Y. Sphingolipid metabolism in brain insulin resistance and neurological diseases. *Front Endocrinol*. 2023;14:1243132. doi:10.3389/fendo.2023.1243132
49. Henríquez-Henríquez MP, Solari S, Quiroga T, Kim BI, Deckelbaum RJ, Worgall TS. Low serum sphingolipids in children with attention deficit-hyperactivity disorder. *Front Neurosci*. 2015;9:300. doi:10.3389/fnins.2015.00300
50. Brunkhorst-Kanaan N, Trautmann S, Schreiber Y, et al. Sphingolipid and endocannabinoid profiles in adult attention deficit hyperactivity disorder. *Biomedicines*. 2021;9(9):1173. doi:10.3390/biomedicines9091173
51. Moruno Manchon JF, Uzor NE, Finkbeiner S, Tsvetkov AS. SPHK1/sphingosine kinase 1-mediated autophagy differs between neurons and SH-SY5Y neuroblastoma cells. *Autophagy*. 2016;12(8):1418–1424. doi:10.1080/15548627.2016.1183082
52. Maceyka M, Harikumar KB, Milstien S, Spiegel S. Sphingosine-1-phosphate signaling and its role in disease. *Trends Cell Biol*. 2012;22(1):50–60. doi:10.1016/j.tcb.2011.09.003
53. Mizugishi K, Yamashita T, Olivera A, Miller GF, Spiegel S, Proia RL. Essential role for sphingosine kinases in neural and vascular development. *Mol Cell Biol*. 2005;25(24):11113–11121. doi:10.1128/MCB.25.24.11113-11121.2005
54. Wu H, Zhang Q, Gao J, et al. Modulation of sphingosine 1-phosphate (S1P) attenuates spatial learning and memory impairments in the valproic acid rat model of autism. *Psychopharmacology*. 2018;235(3):873–886. doi:10.1007/s00213-017-4805-4
55. Rahi V, Kumar P. Animal models of attention-deficit hyperactivity disorder (ADHD). *Int J Dev Neurosci*. 2021;81(2):107–124. doi:10.1002/jdn.10089
56. Kim JW, Sharma V, Ryan ND. Predicting methylphenidate response in ADHD using machine learning approaches. *IJNPPY*. 2015;18(11):pyv052. doi:10.1093/ijnp/pyv052
57. Volkow ND, Wang GJ, Newcorn J, et al. Depressed dopamine activity in caudate and preliminary evidence of limbic involvement in adults with attention-deficit/hyperactivity disorder. *Arch Gen Psychiatry*. 2007;64(8):932. doi:10.1001/archpsyc.64.8.932
58. Neto PR, Lou H, Cumming P, Pryds O, Gjedde A. Methylphenidate-evoked potentiation of extracellular dopamine in the brain of adolescents with premature birth. *N Y Acad Sci*. 2002;965(1):434–439. doi:10.1111/j.1749-6632.2002.tb04184.x
59. Li Y, Ma S, Zhang X, Gao L. ASD and ADHD: divergent activating patterns of prefrontal cortex in executive function tasks? *J Psychiatr Res*. 2024;172:187–196. doi:10.1016/j.jpsychires.2024.02.012
60. Arnsten AFT. The emerging neurobiology of attention deficit hyperactivity disorder: the key role of the prefrontal association cortex. *J Pediatr*. 2010;154(5):I–S43. doi:10.1016/j.jpeds.2009.01.034
61. Bellgrove MA, Mattingley JB, Hawi Z, et al. Impaired temporal resolution of visual attention and dopamine beta hydroxylase genotype in attention-deficit/hyperactivity disorder. *Biol Psychiatry*. 2006;60(10):1039–1045. doi:10.1016/j.biopsych.2006.03.062
62. MacDonald HJ, Kleppe R, Szigetvari PD, Haavik J. The dopamine hypothesis for ADHD: an evaluation of evidence accumulated from human studies and animal models. *Front Psychiatry*. 2024;15:1492126. doi:10.3389/fpsyt.2024.1492126
63. Tong J, McKinley LA, Cummins TDR, et al. Identification and functional characterisation of a novel dopamine beta hydroxylase gene variant associated with attention deficit hyperactivity disorder. *World J Biol Psychiatry*. 2015;16(8):610–618. doi:10.3109/15622975.2015.1036771
64. Polanczyk GV, Willcutt EG, Salum GA, Kieling C, Rohde LA. ADHD prevalence estimates across three decades: an updated systematic review and meta-regression analysis. *Int J Epidemiol*. 2014;43(2):434–442. doi:10.1093/ije/dyt261
65. Jones DN, Raghanti MA. The role of monoamine oxidase enzymes in the pathophysiology of neurological disorders. *J Chem Neuroanat*. 2021;114:101957. doi:10.1016/j.jchemneu.2021.101957

Neuropsychiatric Disease and Treatment

Dovepress
Taylor & Francis Group

Publish your work in this journal

Neuropsychiatric Disease and Treatment is an international, peer-reviewed journal of clinical therapeutics and pharmacology focusing on concise rapid reporting of clinical or pre-clinical studies on a range of neuropsychiatric and neurological disorders. This journal is indexed on PubMed Central, the 'PsycINFO' database and CAS, and is the official journal of The International Neuropsychiatric Association (INA). The manuscript management system is completely online and includes a very quick and fair peer-review system, which is all easy to use. Visit http://www.dovepress.com/testimonials.php to read real quotes from published authors.

Submit your manuscript here: https://www.dovepress.com/neuropsychiatric-disease-and-treatment-journal